Molecular Biology of the Cell
Vol. 20, 4174–4182, October 1, 2009

The Ldb1 and Ldb2 Transcriptional Cofactors Interact with the Ste20-like Kinase SLK and Regulate Cell Migration

Chris J. Storbeck,* Simona Wagner,* Paul O'Reilly,* Marlene McKay,† Robin J. Parks,† Heiner Westphal,‡ and Luc A. Sabourin*†

*Department of Cellular and Molecular Medicine, University of Ottawa, Ottawa, Ontario K1H 8M5, Canada; †Ottawa Hospital Research Institute, Ottawa, Ontario K1Y 4E9, Canada; and ‡Laboratory of Mammalian Genes and Development, National Institute of Child Health and Human Development, Bethesda, MD 20892

Submitted July 10, 2008; Revised July 14, 2009; Accepted July 30, 2009
Monitoring Editor: Martin A. Schwartz

Cell migration involves a multitude of signals that converge on cytoskeletal reorganization, essential for development, immune responses, and tissue repair. Here, we show that the microtubule-associated Ste20 kinase SLK, required for cell migration, interacts with the LIM domain binding transcriptional cofactor proteins Ldb1/CLIM2 and Ldb2/CLIM1/NLI. We demonstrate that Ldb1 and 2 bind directly to the SLK carboxy-terminal AT1-46 homology domain in vitro and in vivo. We find that Ldb1 and -2 colocalize with SLK in migrating cells and that both knockdown and overexpression of either factor results in increased motility. Supporting this, knockdown of Ldb1 increases focal adhesion turnover and enhances migration in fibroblasts. We propose that Ldb1/2 function to maintain SLK in an inactive state before its activation. These findings highlight a novel function for Ldb1 and -2 and expand their role to include the control of cell migration.

INTRODUCTION

Signal transduction events governing cell migration involve an ever-expanding number of molecules functioning in interconnected biochemical pathways. Migration is required for numerous biological processes such as development, tissue repair, and regeneration. In addition to an amino-terminal serine/threonine kinase domain, the Ste20-like kinase SLK bears a central microtubule and nuclear-associated protein (MNAP) homology domain and a carboxy-terminal AT1–46 homology (ATH) domain (Sabourin and Rudnicki, 1999; Sabourin *et al*., 2000), both of unknown function. Elevated SLK expression and activity leads to actin stress fiber dissolution in a Rac1-dependent manner and induction of apoptosis (Sabourin and Rudnicki, 1999; Sabourin *et al*., 2000; Wagner *et al*., 2002). We have previously shown that SLK localizes to vinculin-rich ruffles at the cell periphery in spreading fibroblasts, suggesting a role for SLK in adhesion dynamics (Wagner *et al*., 2002). Importantly, we have shown recently that SLK is activated after scratch-induced migration of fibroblasts (Wagner *et al*., 2008). Expression of kinase defective SLK or small interefering RNA (siRNA) knockdown have shown that SLK is required for efficient cell migration and microtubule-dependent adhesion turnover (Wagner *et al*., 2008). Consistent with a role in cytoskeletal rearrangements, SLK has been shown to indirectly associate with the microtubule network (Wagner *et al*., 2002) and is required for fusion of C2C12 myoblasts (Storbeck *et al*., 2004). Interestingly, SLK has also been shown to regulate cell cycle progression (O'Reilly *et al*., 2005).

This article was published online ahead of print in *MBC in Press* (http://www.molbiolcell.org/cgi/doi/10.1091/mbc.E08–07–0707) on August 12, 2009.

Address correspondence to: Luc A. Sabourin (lsabourin@ohri.ca).

Several LIM domain-containing proteins have roles in cell migration. LIM kinases are required for actin dynamics during directional migration (Nishita *et al*., 2005), and paxillin modulates focal adhesion turnover, a process required for cell migration (Brown and Turner, 2002). Ldb1 (CLIM2, NL1) and the highly related paralogue Ldb2 (CLIM1) (hereafter referred to Ldb1 and Ldb2) are LIM domain binding transcription cofactors required for the function of LIM homeodomain transactivators (Agulnick *et al*., 1996; Jurata *et al*., 1996; Bach *et al*., 1997). Appropriate interactions of these factors are crucial for normal neuronal subtype identity and development (Thaler *et al*., 2002; Mukhopadhyay *et al*., 2003).

Here, we show that the Ldb1/2 coactivators interact with SLK in vitro and in vivo. In addition, we show that siRNA-mediated reduction of Ldb1 and 2 results in a marked increase in migration rate in Boyden chamber haptotaxis assays. Finally, we show that Ldb1 knockdown increases focal adhesion turnover, thus ascribing a novel extranuclear function to Ldb1 and -2 as potential regulators of SLK and cell migration.

MATERIALS AND METHODS

Cell Transfections and Cell Culture

Mouse embryonic fibroblast (MEF) 3T3, NIH 3T3, and primary MEFs were all maintained in DMEM (Invitrogen, Carlsbad, CA) supplemented with 10% fetal bovine serum (Invitrogen), 2 mM L-glutamine (Invitrogen), and penicillin G (200 U ml^{-1}; Invitrogen) and streptomycin sulfate (200 μg ml^{-1}; Invitrogen) in a humidified 37°C incubator at 5% CO_2. DNA transfections into cultured cells were performed using Lipofectamine and Plus reagent (Invitrogen) according to manufacturer's recommendations with a total of 2 μg of plasmid DNA.

Boyden Chamber Migration Assays and Scratch Wound Migration Induction

MEF 3T3 or NIH 3T3 cells were either cotransfected as described with green fluorescent protein (GFP) and deletions of Ldb1 and -2, treated with siRNA to either SLK, Ldb1, Ldb2, or both Ldb1 and -2 and serum starved overnight. Cells were trypsinized the following day, and trypsinization halted with the

addition of soybean trypsin inhibitor (1×; Sigma-Aldrich, St. Louis, MO). Cells (1–3 × 10^4) were resuspended in DMEM containing 0.5% bovine serum albumin and added to the top of a Boyden transwell migration chamber precoated with fibronectin (10 μg ml^{-1}). The cells were then allowed to migrate for 3 h. Residual cells were removed from the top of the chamber, and the filter was rinsed in phosphate-buffered saline (PBS), fixed in 4% paraformaldehyde (PFA) for 10 min, and stained with 4,6-diamidino-2-phenylindole (DAPI) (0.5 μg ml^{-1}; Sigma-Aldrich). The cells that migrated to the underside of the filter were enumerated using DAPI fluorescence. Five to 10 random fields were counted. Cell counts were performed in triplicate for three independent experiments. Representative experiments are shown. Scratch wound-induced migration was performed as described previously (Etienne-Manneville and Hall, 2001). In brief, MEFs were plated on fibronectin (10 μg ml^{-1}), and confluent monolayers were then scratched with pipette tips such that 50% of the monolayer was removed. Cells were then washed with PBS, refed, and collected at various times.

siRNA Knockdown of SLK, Ldb2, and Ldb1

NIH 3T3 cells plated at a density of 3 × 10^5 in 60-mm plates were transfected with 50 or 100 nM siRNA (Dharmacon RNA Technologies, Lafayette, CO) duplex for SLK (5′-GGUUGAGAUUGACAUAUUA), Ldb2 (5′-ACAAGCAGCACGUCCAAUAUU), or Ldb1 (5′-GAACUUAUGUCCCGCCACAUU) by using the Trans-IT TKO (Mirus Bio, Madison, WI) or Lipofectamine 2000 (Invitrogen) transfection reagent according to manufacturer's recommendations. Cells were collected at 48 h after transfection and assayed for cell migration by Boyden chamber and protein expression by Western blot analysis. Control siRNAs consisted of nontargeting duplex (Dharmacon RNA Technologies). Similar results were obtained with scrambled siRNAs.

Plasmid Constructs

DNA plasmids were constructed using standard molecular cloning techniques. Myc-tagged SLK plasmids were constructed as described previously (Sabourin *et al*., 2000). The GST-SLK plasmids were generated by subcloning the corresponding fragments from the Myc-tagged versions (Sabourin *et al*., 2000) to pGEX-5X or 4T1 (GE healthcare, Chalfont St. Giles, Buckinhamgshire, United Kingdom) The yeast two-hybrid SLK-ATH bait plasmid was constructed by inserting the ATH (XhoI digested, blunted with Klenow) domain of SLK in frame with the Gal4 DNA binding domain in pAS2 (Clontech, Mountain View, CA). Ldb1 and -2 were excised from pACT2 (XhoI/EcoRI) and subcloned in frame into Myc and hemagglutinin (HA) epitope-tagged vectors (pCAN-HA or pCAN-Myc). The following Ldb2 constructs were generated by excising fragments of Ldb2 from HA-Ldb2 and recloning into pCAN-HA: HA-Ldb2 ΔLBD (aa 1–296), HA-Ldb2 DD (aa 1–186), HA-Ldb2 nuclear localization signal (NLS) (aa 188–288), and HA-Ldb2 DDΔC (aa 1–124). HA-Ldb2 LBD (aa 298–373) was generated by polymerase chain reaction (5′-gggggatccagctgcaaacctgagtctgtcc-3′ and 5′-gggggaattcacgggcctattgacagtggattct-3′) using VENT polymerase (New England Biolabs, Ipswich, MA). All clones were verified by DNA sequencing.

Antibodies and Immunofluorescence

The primary antibodies used in these studies were as follows: SLK polyclonal antibodies were as described previously (Sabourin *et al*., 2000), Ldb1 (Santa Cruz Biotechnology, Santa Cruz, CA), α-tubulin (Sigma-Aldrich), and Ldb2 (Abcam, Cambridge, MA). For immunofluorescence studies, the cells were plated on coverslips coated with fibronectin (10 μg/ml) and incubated overnight. Cells were then rinsed with PBS, fixed in 4% PFA, and blocked in PBS containing 5% goat or donkey serum and 0.3% Triton X-100 for 20 min. Fresh blocking solution containing primary antibody was added and incubated for 1 h at room temperature. Antibodies were detected with either anti-mouse, anti-goat, or anti-rabbit secondaries conjugated to either fluorescein isothiocyanate or tetramethyl rhodamine isothiocyanate (Sigma-Aldrich). The samples were visualized with an LSM5 laser scanning confocal microscope (Carl Zeiss, Thornwood, NY) equipped with the appropriate filters and photographed with a digital camera (HB050; Sony, Tokyo, Japan) by using the LSM5 Pascal software package.

For live imaging analysis, 1–5 × 10^4 MEF 3T3 cells were transfected with 1.5 μg of GFP paxillin, siGlow (Dharmacon RNA Technologies) tracker, and either control siRNA or siRNA specific for Ldb1 by using lipofectamine 2000 as per the manufacturer's instructions. Live imaging was performed using a laser scanning confocal microscope (LSM5 Pascal; Carl Zeiss) with a heated stage (37°C) at 5% CO_2. Dual-fluorescent images were captured using the Pascal software package for GFP paxillin and siGlow at emission spectra of 488 and 543 nm, respectively. Images were obtained once per minute for 10 min. Focal adhesion brightness quantitation was performed using ImageJ software (National Institutes of Health, Bethesda, MD), and dissociation constants were calculated as described previously (Webb *et al*., 2004).In brief, the ratio of GFP fluorescence intensity at time (t) 0 and at t = X was calculated after background subtraction. The natural log of this quotient ($\ln[I_o/I_t]$) was then plotted over time, and the slope was calculated to obtain K*diss*(min^{-1}). At least 20 focal adhesions were analyzed from three different cells for the control and siLdb1 treatments.

Western Blotting and Immunoprecipitation and Kinase Assays

Cells were lysed in radioimmunoprecipitation assay buffer as described previously (O'Reilly *et al*., 2005), and lysates were cleared by centrifugation at 10,000 × *g* for 2 min. Protein concentrations were determined using protein assay dye reagent (Bio-Rad Laboratories, Hercules, CA). Equal amounts of protein (20–40 μg) were electrophoresed on 8–15% polyacrylamide gels and transferred to polyvinylidene difluoride (PVDF) membrane. Membranes were probed with the indicated antibodies overnight at 4°C in 5% skim milk powder in 1× Tris-buffered saline/Tween 20 (TBST; 50 mM Tris, pH 7.4, 150 mM NaCl, and 0.05 Tween 20). Membranes were washed in TBST and incubated with horseradish peroxidase-coupled secondary antibodies, and the reactive proteins were detected using chemiluminescence (PerkinElmer Life and Analytical Sciences, Boston, MA) and exposure to x-ray film.

For immunoprecipitations, 300 μg of protein lysate was immunoprecipitated with 2–3 μg of antibody and 20 μl of protein A-Sepharose (GE Healthcare) for 2–12 h. Immunocomplexes were recovered by centrifugation and washed with NETN buffer (20 mM Tris-HCl, pH 8.0, 1 mM EDTA, 150 mM NaCl, and 0.5% Nonidet P-40) and subjected to SDS-polyacrylamide gel electrophoresis (PAGE) or kinase assay. In vitro SLK kinase assays were performed after SLK immunoprecipitation as described previously (O'Reilly *et al*., 2005). Kinase reactions were stopped by adding 7 μl of 4× SDS sample buffer and electrophoresed on 8% SDS-PAGE. The gels were transferred to PVDF membranes and subjected to autoradiography followed by Western blotting with SLK antibody.

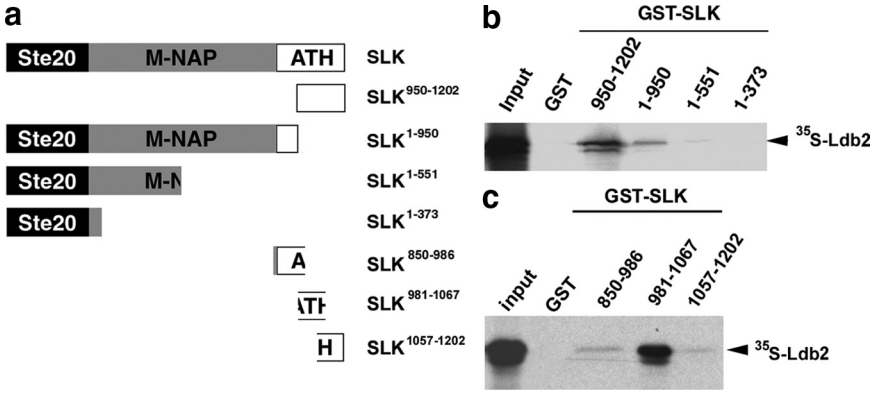

Figure 1. Ldb1 and -2 associate with the ATH domain of SLK. (a) SLK deletion mutants include the ATH domain ($SLK^{950–1202}$), a deletion lacking most of the ATH domain ($SLK^{1–950}$) or lacking half the MNAP and the entire ATH domain ($SLK^{1–551}$), the kinase domain alone ($SLK^{1–373}$) and subdomains of the ATH (aa 850–986, aa 981-1067, and aa1057–1202). (b) Binding of in vitro translated Ldb2 to GST-SLK deletions (see a). GST-SLK fusions were incubated with ^{35}S-labeled Ldb2, washed, and bound Ldb2 was detected by SDS-PAGE and autoradiography. GST proteins were analyzed separately by SDS-PAGE and Coomassie staining (data not shown). Ldb1 binds preferentially to the SLK ATH domain in vitro, supporting a direct interaction between Ldb1 and SLK. (c) Mapping of the Ldb2 binding domain within the ATH domain (aa 950-1202) of SLK. SLK deletion mutants encompassing the MNAP and ATH domains (see a) were assayed for binding to Ldb2 as described in b. Ldb2 bound almost exclusively to GST-ATH-981-1067, indicating that it binds preferentially to the central region of the SLK ATH domain. Identical results were obtained with Ldb1 (data not shown).

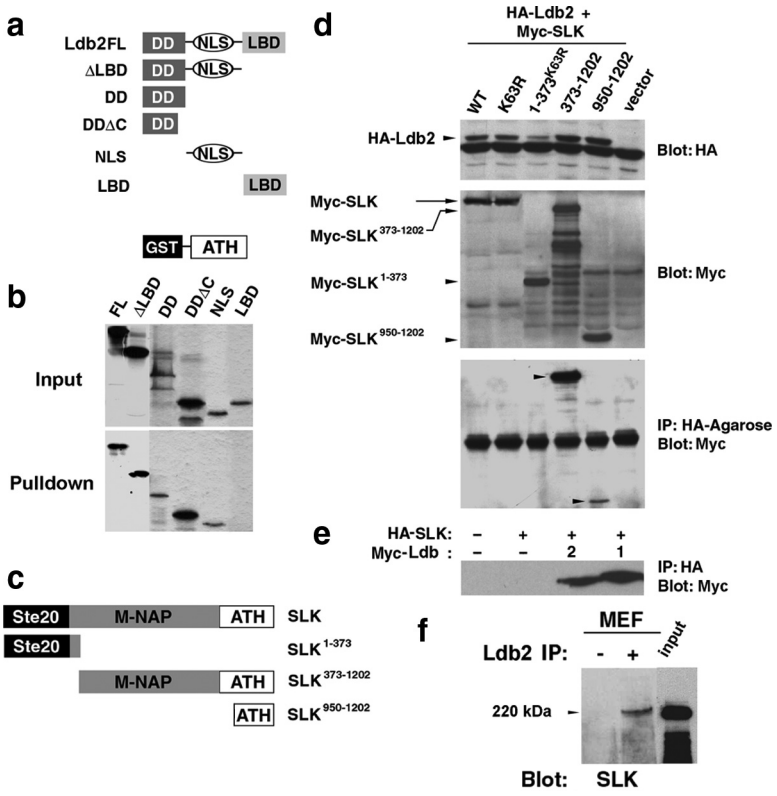

Figure 2. SLK and Ldb association in vitro and in vivo. (a) Domain organization and schematic representation of Ldb1/2 deletion constructs. Ldb proteins contain an amino-terminal DD, a central domain containing a NLS, and a carboxy-terminal LIM binding domain (LBD). Full-length Ldb2 (Ldb2 FL; full length) and various deletion mutants are indicated, including the Ldb2 LIM binding domain (LBD; aa 298–373), Ldb2 lacking the LIM binding domain (Ldb2 ΔLBD; aa 1–296), versions of the Ldb2 dimerization domain (Ldb2 DD; aa 1–186 and DDΔC; aa 1–124), and the Ldb2 nuclear localization signal domain (Ldb2 NLS; aa 188–288). (b) Association of Ldb2 deletion mutants with the SLK ATH domain. Ldb2 mutants were translated in the presence of [^{35}S]methionine and subjected to a binding assay with GST-ATH as described in text. The Ldb2 dimerization domain and the NLS domain could independently bind the SLK ATH domain, suggesting a strong interaction between the two factors. No binding was observed to the LIM-binding domain. (c) Schematics of Myc epitope-tagged SLK deletion mutants. Full-length SLK (SLK), the kinase domain alone (SLK 1–373), SLK lacking the kinase domain (SLK 373-1202) and the SLK ATH domain (SLK 950-1202) are shown. (d) Cotransfection of HA-tagged Ldb2 and Myc-tagged SLK deletion constructs was performed in human embryonic kidney 293 cells. Extracts were immunoprecipitated with anti-HA antibody (12CA5) and immunoblotted with anti-Myc antibody (9E10) (bottom). Expression of the transfected constructs was confirmed by Western blotting (top and middle). Only Myc-SLK$^{373–1202}$ and Myc-SLK$^{950–1202}$ coprecipitated with HA-Ldb2, suggesting that the ATH domain is required and that the kinase domain interferes with anti-HA coprecipitation of Myc-SLK and HA-Ldb2. (e) Reciprocal co-IP showing that full-length HA-SLK associates with Myc-Ldb1 and 2. (f) Association of endogenous SLK and Ldb. Ldb2 was immunoprecipitated from protein lysates obtained from MEF cells. A 220-KDa band corresponding to SLK coprecipitated with Ldb2. As a control for nonspecific binding to the Sepharose beads, protein A-Sepharose beads alone were added to 400 μg of the same protein lysates. Similar results were obtained with Ldb1.

In Vitro Binding Assays

Glutathione transferase (GST) fusion proteins were generated by induction of bacterial cultures with 1 mM isopropyl β-D-thiogalactoside (IPTG; Sigma-Aldrich) for 2 h. Bacteria were pelleted, resuspended in 1 ml of bacterial lysis buffer (20% sucrose, 10% glycerol, 50 mM Tris-HCl, pH 8.0, 2 mM $MgCl_2$, 2 mM dithiothreitol, 10 μg ml^{-1} leupeptin, 10 μg ml^{-1} pepstatin, 10 μg ml^{-1} aprotinin, 1 mM phenylmethylsulphonylfluoride, and 100 μM benzamidine) and sonicated on ice. Glutathione-Sepharose beads (GE Healthcare) were added to the cleared supernatants, and bound GST fusions were collected by centrifugation, washed three times with NETN, and subjected to binding assays. In vitro translated proteins were generated using the TNT quick-coupled in vitro transcription translation kit (Promega, Madison, WI) according to the manufacturer's instructions. Translated proteins were incubated with either GST or GST fusions in NETN buffer, washed with NETN, and eluted from the beads by boiling in sample buffer. Proteins were fractionated by SDS-PAGE, the gels were stained with Coomassie Brilliant Blue (Sigma-

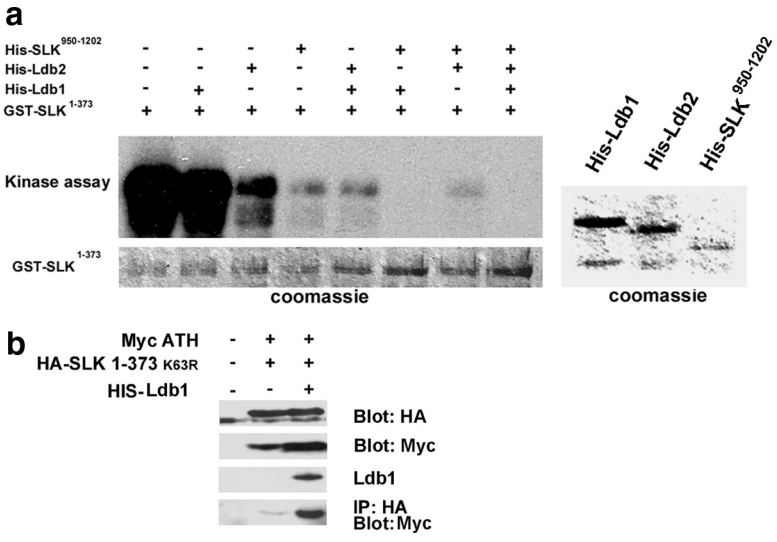

Figure 3. Ldb1 and -2 inhibition of SLK in vitro and activation of SLK in transfected cells. Effect of Ldb1 and -2 on SLK activity in vitro and in vivo. (a) Recombinant GST-SLK$^{1–373}$ autocatalytic activity is inhibited when incubated with combinations of recombinant His-tagged Ldb1, Ldb2, and SLK ATH domain (SLK$^{950–1202}$). The input HIS-fusions are shown in the right panel. (b) When coexpressed in 293, His-Ldb1 increases the efficiency of coprecipitation of the SLK kinase domain with the ATH region. Myc-tagged SLK ATH domain coprecipitates HA-tagged SLK kinase domain. Inclusion of His-tagged Ldb1 increases the amount of Myc-ATH recovered in coimmunoprecipitations, suggesting that Ldb1 can facilitate "bridging" of the kinase and ATH domains of SLK.

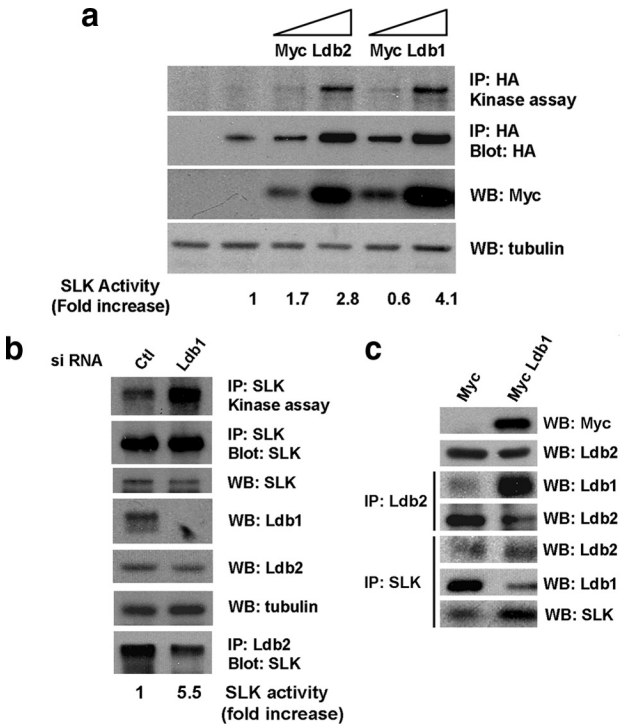

Figure 4. Control of SLK activity by Ldb expression. (a) Expression of Myc-Ldb1 and -2 results in activation of HA-SLK. HeLa cells were transfected with 1 μg of HA SLK plasmid and 1 or 3 μg of Myc-Ldb1 or 2 plasmids. SLK was precipitated with an HA antibody (12CA5), and kinase assay was performed. Increasing amounts of Ldb factors result in elevated SLK activity. (b) Increased SLK activity with siRNA-mediated ablation of Ldb1 in MEF 3T3 cells. MEF 3T3 cells were treated with Ldb1 siRNA and near complete reduction of Ldb1 was seen. No change in expression of Ldb2, SLK or tubulin (control) was observed. However, a reduction in the amount of Ldb2 coimmunoprecipitating with SLK was noted. In the absence of Ldb1, SLK activity was activated 5.5-fold, suggesting that Ldb1 functions to maintain an inhibitory complex with Ldb2 and SLK. (c) Overexpression of Myc-Ldb1 alters the Ldb-SLK complex. Cells overexpressing Myc-Ldb1 as described in a were subjected to immunoprecipitations and Western blot analysis. Overexpression of Myc-Ldb1 was found to alter the endogenous SLK–Ldb1 complex.

Aldrich) to visualize the proteins, destained (30% methanol and 10% acetic acid), dried, and subjected to autoradiography.

Recombinant SLK was prepared by inducing an overnight culture of GST-SLK with IPTG and preparing GST SLK as described above. Recombinant His-tagged Ldb1, Lbd2, and SLK ATH domain ($SLK^{950-1202}$) were prepared by inducing overnight cultures with IPTG and purifying recombinant protein through nickel-nitrilotriacetic acid columns (QIAGEN, VALENICA, CA) according to manufacturer's instructions. Kinase assays were performed as described above.

Yeast Two-Hybrid Analysis

Yeast two-hybrid screens were performed as suggested by the manufacturer (Clontech). In brief, the ATH domain of SLK was subcloned into pAS2, in frame with the GAL4-DBD as described above. Yeast strain AH109 (Clontech) was transformed and tested for self-activation by using the endogenous LacZ reporter and His auxotrophy. The resulting AH109 clones were mated with library (mouse E10.5 cDNA) pretransformed Y187, and His/Trp/Leu auxotrophs were screened for positive interaction. Of the resulting 29 clones, five clones contained the Ldb1 cDNA and three clones contained the Ldb2 cDNA. cDNAs were subcloned into HA- or Myc-tagged vectors and further tested for ATH binding.

RESULTS

Ldb1 and 2 Interact with SLK ATH Domain

We have shown previously that SLK induces cytoskeletal rearrangements through a Rac1-mediated pathway (Wagner *et al.*, 2002). Recently, we have shown that SLK is required for motility and is activated after scratch-induced migration in fibroblasts (Wagner *et al.*, 2008). Our previous studies have demonstrated that deletion of the SLK ATH domain increases its kinase activity, suggesting that it plays a role in SLK regulation (Sabourin *et al.*, 2000). To gain further insight into the autoinhibitory role of the ATH domain, we performed a yeast two-hybrid screen with a GAL4-DBD-ATH domain fusion as bait. Surprisingly, we identified the transcription cofactors Ldb1 and Ldb2 as ATH-interacting proteins (Supplemental Figure 1). Interestingly, Ldb factors (reviewed in Matthews and Visvader, 2003) are LIM binding domain transcriptional cofactors. We initially sought to confirm the interaction of Ldb1 and -2 with the SLK-ATH domain in yeast. Ldb1 and -2 interacted with the ATH-GAL4-DBD fusion but not the GAL4-DBD, indicating that the Ldb factors associate specifically with the ATH domain (Supplemental Figure 1). Similarly, patching of these clones in a β-galactosidase reporter assay resulted in the activation of the LacZ reporter gene (Supplemental Figure 1).

Interactions of Ldbs and SLK were confirmed by direct binding assays. In vitro-translated full length Ldbs labeled with [^{35}S]methionine were incubated with various GST-SLK fusion protein deletions (Figure 1). After pulldowns, Ldb2 had the highest affinity for the SLK ATH domain ($SLK^{950-1202}$; Figure 1B) and moderate affinity for a carboxy-terminal deletion of SLK lacking the latter two thirds of ATH domain

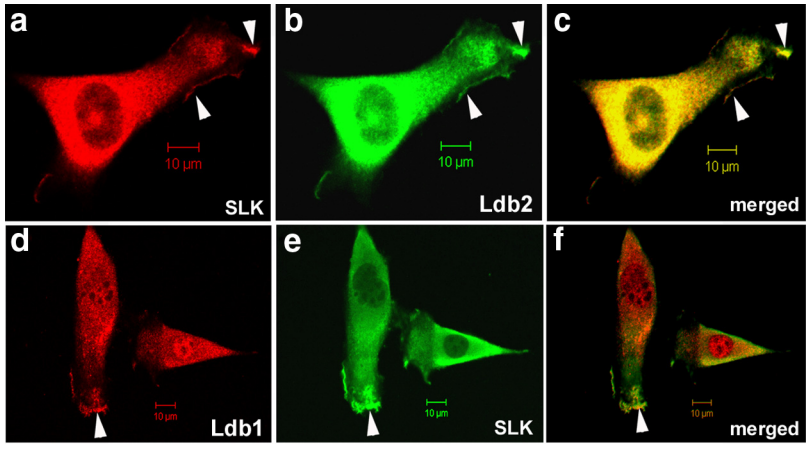

Figure 5. Detection of SLK, Ldb1, and Ldb2 in leading edge ruffles and microtubules. Colocalization of SLK (a and e) with Ldb2 (b) or Ldb1 (d) in membrane ruffles and leading edge of migrating fibroblasts on fibronectin (a–c; arrowhead) or C2C12 myoblasts (d–f). Images were acquired with an LSM5 confocal microscope. Bar, 10 μm.

(SLK$^{1–950}$). Prolonged exposures also revealed weak binding to deletions of SLK lacking the ATH domain (GST-SLK-1-551, GST-SLK-1-373). To refine the binding region of SLK to Ldb2, GST fusions (Figure 1A) of the SLK ATH domain were assayed for binding to ^{35}S-labeled Ldb2 (Figure 1C). Binding of Ldb2 to the ATH amino-terminal third (SLK$^{850–986}$) and the ATH carboxy-terminal third (SLK $^{1057–1202}$) was minimal. Strong binding to an 86-amino acid stretch of the ATH central region (SLK$^{981–1067}$) was observed indicating that Ldb2 binds this region of SLK with highest affinity (Figure 1C). Ldb1 was also able to bind directly to the SLK-ATH domain in vitro in a manner that was indistinguishable from Ldb2 (data not shown). Together, these data indicate that both Ldb1 and -2 preferentially target the ATH domain of SLK in vitro.

To map the Ldb1/2 domains of interaction, ^{35}S-labeled deletions of Ldb2 were assayed for binding to a GST-tagged SLK ATH domain (Figure 2A). Interestingly, a 186-amino acid portion of the dimerization domain (DD) and a 100-amino acid fragment of the NLS region of Ldb2 could independently bind the SLK ATH domain in vitro (Figure 2B). In addition, versions of Ldb2 lacking the C-terminal LIM binding domain (ΔLBD) were able to bind the SLK ATH domain, whereas the LBD of Ldb2 by itself could not (Figure 2B). Further deletion of 62-amino acids from the carboxy-terminal end of the dimerization domain (DDΔC) retained binding thus refining the Ldb2 binding region to the SLK ATH domain in the N-terminal 124 amino acids of Ldb2. An analogous set of Ldb1 deletion mutants were tested for binding to GST-ATH with similar results (data not shown). Therefore, Ldb1 and -2 probably contact the central region of the SLK ATH domain through both their dimerization and NLS domains.

Association of Ldb1 and -2 with SLK In Vivo

We next tested whether Ldb1 and -2 were able to bind the SLK ATH domain in cultured cells. To address this, HA-tagged Ldb2 and Myc-tagged SLK deletion constructs (Figure 2C) were cotransfected into 293 cells and subjected to immunoprecipitation and Western blot analysis (Figure 2D). After coimmunoprecipitation analyses, Myc-tagged SLK deletion constructs containing the ATH domain (Myc SLK$^{373–1202}$ and Myc SLK$^{950–1202}$) were found to coprecipitate with HA-Ldb2. Similarly, HA-Ldb1 could also be coprecipitated with these SLK truncations (data not shown). Surprisingly, full-length SLK and kinase inactive (Myc-SLK, Myc-SLK K63R) did not coimmunoprecipitate with HA-Ldb2. This suggests that the presence of the SLK kinase domain either masks the interaction between the ATH domain and Ldb2 or, alternatively, renders the epitope tag on Ldb2 inaccessible to the antibody. To address the latter possibility, we used HA-tagged SLK and Myc-tagged Ldb1 and -2 and repeated the coimmunoprecipitations. Indeed, Myc-tagged Ldb1/2 could be detected in HA–SLK immune complexes, suggesting that the amino termini of the Ldb factors are inaccessible to antibody when in complex with SLK (Figure 2E). Supporting the cotransfection data, endogenous Ldb1 was also found to coprecipitate with SLK in immunoprecipitation (IP)-Western blot analyses using lysates from fibroblasts (Figure 2F). Together, these experiments confirm that the ATH domain of SLK is required for interaction with Ldb1 and 2 in vivo.

Effects of Ldb1 and -2 on SLK Activity In Vitro and In Vivo

We next investigated the effect of Ldb molecules on SLK activity in vitro (Figure 3A). Although Ldb2 was more effective, both Ldb1 and -2 could inhibit the activity of

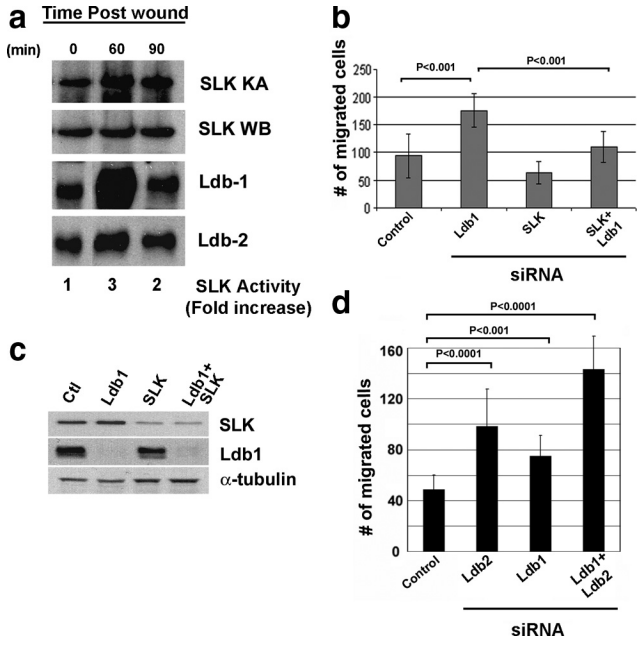

Figure 6. Knockdown of Ldb1/2 enhances cell migration. (a) Confluent MEF3T3 cells were scratch wounded and subjected to SLK kinase assays. The IPs were also blotted for Ldb1, Ldb2, and SLK. Kinase activity was evaluated by densitometric scanning and normalized to total SLK levels. A shift toward increased Ldb1 association correlates with SLK activation. (b) MEF3T3 cells were treated with control siRNA or siRNAs to Ldb1, SLK, or both and assayed for protein levels by Western blot analysis. Efficient knockdown of Ldb1 was achieved, whereas SLK levels were reduced by ~75%. (c) The same cultures were analyzed for migration potential in a transwell migration assay. Reduction of Ldb1 levels enhanced cell motility whereas reduction of SLK reduced motility. Reduction of both Ldb1 and SLK resulted in restoration of normal motility, suggesting that enhanced migration in the absence of Ldb1 is SLK dependent. (d) Reduction of Ldb1 and Ldb2 results in a fourfold enhancement of cell migration. As shown above, reduction of Ldb1 resulted approximately a 1.5-fold enhancement in motility whereas reduction of Ldb2 enhanced motility by approximately twofold. Reduction of both Ldb1 and -2 resulted in an additive fourfold enhancement of cell motility, suggesting that these two factors function together with SLK to control cell migration. Ldb1 and -2 knockdowns were performed as described above and protein levels were evaluated by Western blot.

GST-SLK$^{1–373,}$ an SLK truncation lacking the C-terminal region (Figure 3A). In agreement with a reported inhibitory role of the ATH domain on SLK activity (Sabourin *et al*., 2000), recombinant His-tagged SLK ATH domain (His-SLK$^{950–1202}$) could suppress SLK$^{1–373}$ activity dramatically. Both Ldb factors added alone or together also markedly reduced SLK$^{1–373}$ activity. When combined with the SLK ATH domain (SLK$^{950–1202}$), addition of either Ldb1 or Ldb2 resulted in further reductions of SLK$^{1–373}$ kinase activity (Figure 3A). These results suggest that Ldb1/2 can enhance or stabilize the negative regulation imparted by the ATH on the kinase domain. Supporting this, the ATH and SLK kinase domain (1–373) can be coprecipitated much more efficiently in the presence of Lbd1 (Figure 3B). Together, these data suggest that the Ldb molecules can inhibit SLK activity. Furthermore, the interaction of the kinase domain with the ATH is likely to be stabilized by the Ldbs, resulting in strong SLK inhibition.

To investigate the role of the Ldbs in cells, we expressed increasing amounts of Myc-tagged Ldb molecules with HA-

tagged SLK (Figure 4A). After normalization to immunoprecipitated SLK, expression of incremental amounts Ldb1 and -2 resulted in increased SLK activity compared with HA-SLK alone (Figure 4A). One possibility is that increased expression of Ldb factors alters the stoichiometry of the Ldb/SLK complex, resulting in elevated SLK activity.

To further examine the relevance of the Ldb1/SLK association, we ablated Ldb1 from MEF 3T3 cells by using siRNA specific for Ldb1 (Figure 4B). Although Western blot analysis revealed no change in Ldb2 or SLK expression, Ldb1 levels were reduced to near undetectable levels. Surprisingly, siRNA-mediated down-regulation of Ldb1 in MEF 3T3 cells resulted in a 5.5-fold elevation of SLK activity after normalization to immunoprecipitated SLK. Furthermore, down-regulation of Ldb1 resulted in a reduction of Ldb2 association with SLK (Figure 4B), suggesting that Ldb1 may play a role in the assembly or stability of the complex. Nonetheless, consistent with an inhibitory role for the Ldb molecules on SLK activity, ablation of Ldb1 results in loss or reduction of both Ldb factors from the SLK complex and increased SLK activity.

Surprisingly, overexpression and down-regulation of the Ldbs has the same effect on SLK activity. Because we have found that the Ldbs can heterodimerize (Supplemental Figure 2), we investigated whether a titration effect by the overexpressed Ldb factors could be responsible for this phenomenon. Cells overexpressing Myc-Ldb1 and showing increased SLK activity (Figure 4A) were subjected to various immunoprecipitation experiments. As shown in Figure 4C, overexpression of Myc-Ldb1 results in a marked increase in the amount of Ldb1 that can be coprecipitated with Ldb2, suggesting that the endogenous Ldb2 can associate with the exogenous Ldb1 in a complex stoichiometry. Importantly, overexpression of Myc-Ldb1 resulted in a loss of SLK-associated Ldb1, probably through dimerization with Myc-Ldb1. Therefore, both overexpression and knockdown of the Ldbs result in a loss of SLK-bound Ldbs, thereby increasing SLK kinase activity.

Ldb Proteins Colocalize with SLK in Migrating Cells

We have established that Ldb factors can associate with the ATH domain of SLK in vitro and in vivo and function to regulate SLK activity. We then sought to investigate the distribution of the SLK/Ldb complex in migrating cells. We performed confocal microscopy of endogenous Ldb1/2 and SLK in MEFs (Figure 5). Ldb2 and SLK were observed to colocalize at leading edge structures (arrowheads, Figure 5, A–C) of MEFs. This was also observed for Ldb1 in C2C12 myoblasts (arrowheads, Figure 5, D–F). These data suggest that Ldb1 and -2 colocalize with SLK at the leading edge consistent with a role for these factors in SLK regulation and cell migration.

Alteration of Ldb Levels Increases Cell Migration

The observation that Ldb factors may regulate SLK activity in vivo prompted us to examine the endogenous complex upon SLK activation during scratch induced migration. NIH 3T3 cells were scratch wounded (Etienne-Manneville and Hall, 2001) and SLK activity and Ldb1/2 association was monitored. Interestingly, higher SLK activity (Figure 6A) was accompanied by a marked increase in SLK-associated Ldb1, with little or no change in the levels of SLK-associated Ldb2. This suggests that the stoichiometry of the complex is modulated during cell migration in vivo, probably toward increased Ldb1 association, resulting in SLK activation.

We have shown previously that SLK knock down inhibits cell migration (Wagner *et al*., 2008), and we sought to address the role of Ldb1 in this process. After siRNA treatment, the levels of Ldb1 protein were markedly reduced whereas SLK levels were down-regulated by ~75% (Figure 6B). Reducing Ldb1 levels resulted in approximately a two-fold increase in cell migration, whereas reduced cell migration was observed with a knockdown of SLK (Figure 6C). Reduction of both Ldb1 and SLK restored the migration potential of the cells to basal levels, suggesting that the Ldb1-mediated effect on cell migration is SLK dependent (Figure 6C).

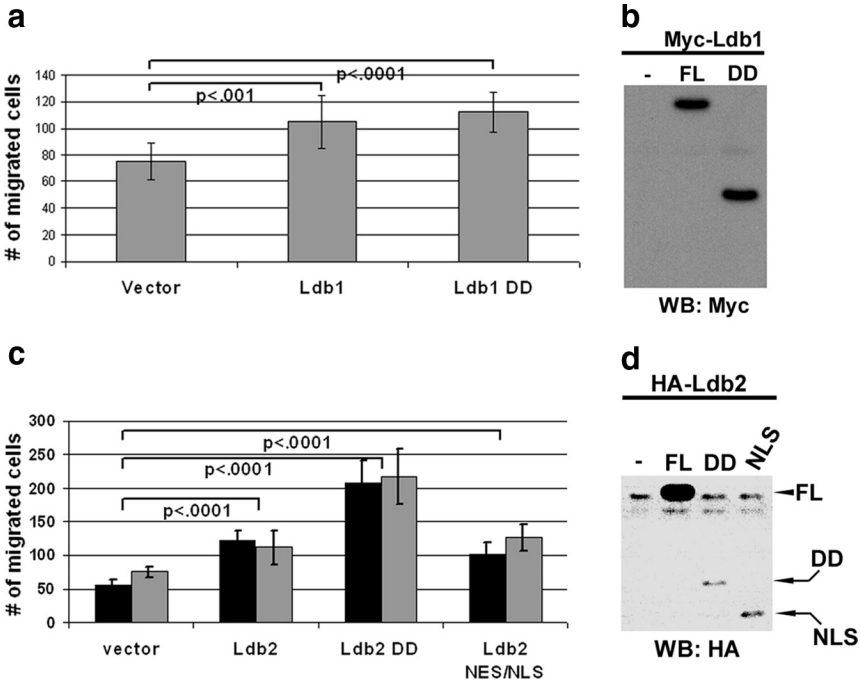

Figure 7. Overexpression of Ldb1/2 also enhances cell migration. (a) Confluent Cells were cotransfected with GFP and full-length Ldb2 or the DD and assessed for motility of GFP-positive cells in a transwell assay. Overexpression of Ldb1 or the dimerization segment increased cell migration, suggesting that normal expression levels of Ldb factors are crucial for normal migration and that the dimerization domain of Ldb1 can function as a dominant negative. (b) Western blot analysis shows expression of the Myc-Ldb1 constructs. (c) Overexpression of Ldb2 constructs also increases cell motility. Migration was assessed as in described in a, and the two sets of bars represent two independent transfection experiments. Expression of the DD markedly increased cell motility. (d) Western blot analysis indicating expression of HA-Ldb2, HA-Ldb2DD, and HA-Ldb2-NLS. Arrowheads indicate the various protein products.

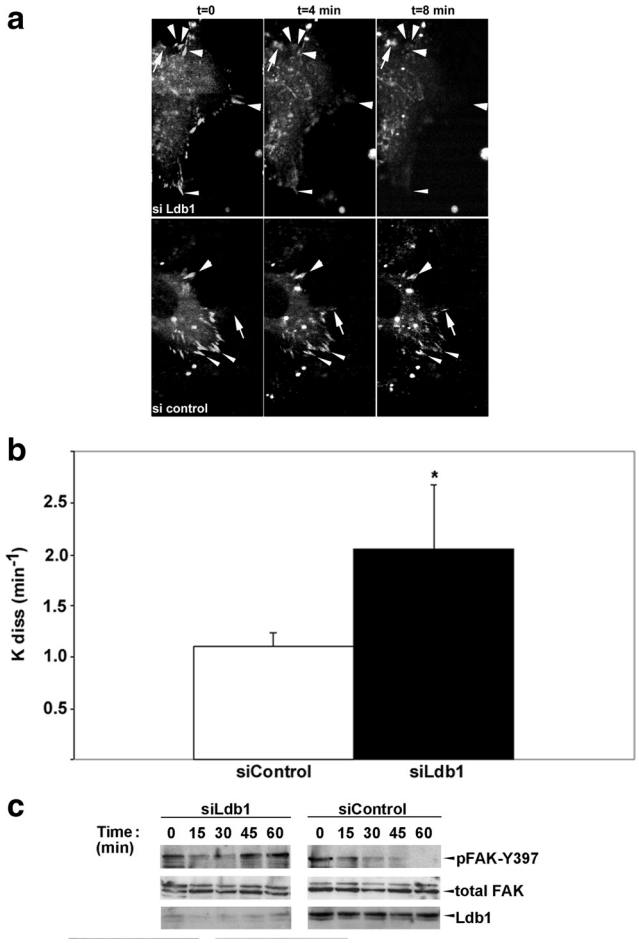

Figure 8. Knockdown of Ldb1 increases focal adhesion turnover. (a) MEF3T3 cells were cotransfected with siLdb1, siGlow tracker, and GFP-paxillin. The cells were then monitored for red (siGlow) and green (GFP) fluorescence. Double-positive cells were subjected to live imaging as described in *Materials and Methods*. (b) Focal adhesion disassembly constants were calculated as described (Webb *et al*., 2004). A twofold increase in turnover (1.11 vs. 2.1 min^{-1}; $p < 0.0001$) was observed for siLdb1-transfected cells. Significance to $p < 0.0001$ is indicated by the asterisk (*). (c) NIH 3T3 cells transfected with Ldb1 siRNAs were subjected to nocodazole washouts and analyzed for FAK-pTyr397 levels. The kinetics of turnover in Ldb1 knockdowns were faster that that observed in control cultures as evidenced by focal adhesion reassembly at 45 min.

Next, we analyzed the effect of both Ldb1 and -2 knockdown on cell migration. A marked reduction of Ldb1 can be achieved. However, thus far, we can only reduce Ldb2 levels to ~50% of control (data not shown). Nevertheless, reduction of Ldb1 again resulted in approximately a 1.5-fold increase in cell migration, whereas reduction of Ldb2 led to approximately a twofold increase in cell migration (Figure 6D). However, when both Ldb1 and -2 were reduced, an almost fourfold enhancement of cell migration was observed (Figure 6D).

Previous studies in *Drosophila* have shown the importance of stoichiometry for Ldb function in that overexpression of the *Drosophila* Ldb orthologue Chip is a phenocopy of the Chip knockout fly (Fernandez-Funez *et al*., 1998; Rincon-Limas *et al*., 2000). We therefore investigated the effect of Ldb1 or Ldb2 overexpression on cell migration. Ldb1 overexpression resulted in an approximately twofold enhancement in migration compared with control-transfected cells, whereas expression of the Ldb1 dimerization domain (Ldb1DD), binding to SLK, resulted in approximately a fourfold increase in migration (Figure 7A). Similarly, overexpression of Ldb2 or domains binding the ATH significantly increased cell motility (Figure 7C). The presence of Ldb polypeptides was confirmed by Western blot (Figure 7, B and D). For unknown reasons, the LIM binding domains could not be expressed at any detectable levels and could not be tested. However, the expression levels of the transfected constructs were severalfold higher than the endogenous proteins (Supplemental Figure 3). As for the *Drosophila* system, these data suggest that expression of Ldb1 or Ldb2 probably influences the overall stoichiometry of the SLK–Ldb complex and hence cell migration.

Our previous results have shown that expression of dominant negative SLK impairs focal adhesion turnover (Wagner *et al*., 2008). Therefore, we tested the effect of Ldb1 knockdown on focal adhesion turnover by using GFP-paxillin as a reporter. As shown in Figure 8A, focal adhesion disassembly, as measured by GFP-paxillin fluorescence, proceeded markedly faster in siLdb1-treated cells. Disassembly constant calculations revealed a twofold increase in adhesion turnover rate for siLdb1-transfected cells (Figure 8B). Supporting these data, knock down of Ldb1 in NIH 3T3 cells resulted in faster focal adhesion turnover in nocodazole washout experiments (Figure 8C). Whereas Ldb1 siRNA treated cells reassembled focal adhesions ~45 min after washout, control-treated cells did not show reassembly for up to 60 min. Together, these data suggest that critical control of SLK/Ldb stoichiometry is required for controlled cell migration, possibly by regulating SLK activity.

DISCUSSION

Ldb1 and -2 Association with SLK

Our results show that Ldb1 and -2 associate with the ATH domain of SLK in vitro and in vivo. Both the dimerization and NLS domains of Ldb1 and -2 independently bind the SLK ATH domain in vitro, suggesting a multicontact association between these proteins. Because the Ldb factors are not substrates for SLK and that depletion of Ldb1 did not affect the intracellular distribution of SLK (data not shown) we propose that their association with SLK is probably to control its activity. However, our results suggest that the stoichiometry of this association is quite complex and seems to be dynamic.

It has been recently suggested that SLK can form homodimers (Pike *et al*., 2008; Storbeck, unpublished). In LIM homeodomain transcription factors, an Ldb1 homodimer is required to link two of these proteins in a functional complex (van Meyel *et al*., 2000; Thaler *et al*., 2002). Therefore, we propose that an Ldb1/2 heterodimer can form a tetrameric complex with two SLK molecules. The observation that tagged versions of Ldb1 and -2 can be coimmunoprecipitated suggests that these factors can heterodimerize (Supplemental Figure 2). The enhanced migration and SLK activity observed with both Ldb1 knockdown and overexpression may result from altering the balance of Ldb factors required for appropriate SLK function. Indeed, our results show that overexpression Myc-Ldb1 results in a loss of SLK-associated Ldb1, suggesting a titration effect in overexpressing cells. A similar phenomenon has been observed with the drosophila Ldb homologue Chip in controlling the LIM homeodomain transcription factor Apterous (Fernandez-Funez *et al*., 1998; Rincon-Limas *et*

al., 2000). Interestingly, in agreement with our observation that expression of Ldb1 enhances migration in a Boyden chamber assay (Figure 7), increased Ldb1 levels have been detected by immunohistochemistry at the peripheral region of oral carcinomas, an area of the tumor correlating with increased motility (Mizunuma *et al*., 2003).

Our observations show that recombinant Ldb factors in combination with recombinant SLK ATH domain can completely inhibit SLK^{1-373} (SLK kinase domain) activity (Figure 3A). It is then possible that Ldb association controls SLK activity by sequestering the kinase domain in a complex with the SLK ATH domain and the Ldb dimerization domain. This structural arrangement is suggested by the observation that the Ldb proteins can enhance the formation of a tripartite association between Ldb/ATH and the kinase domain when coexpressed as individual domains (Figure 3B). Further evidence to support a role for the Ldb factors in controlling SLK activity comes from Ldb1 siRNA experiments demonstrating a 5.5-fold increase in SLK activity when Ldb1 is deleted (Figure 4B). In addition, reduced association of Ldb2 with SLK observed in the absence of Ldb1 suggests that a full complement of both Ldb factors is required for negative regulation of SLK (Figure 4B). It is possible that SLK dimers may form a low activity complex with an Ldb1/2 heterodimer. A shift from Ldb1/2 heterodimers complexed with SLK to more Ldb1 homodimers in complex with SLK may occur during migration, modulating SLK activity. Posttranslational modification of Ldb1/2 or SLK might shift the stoichiometry of the complex, resulting in SLK activation. Interestingly, overexpression of Ldb1 or Ldb2 results in increased SLK activity and motility. It is then probable that this results in a titration of SLK-bound Ldb molecules, increasing SLK activity. We are currently using crystallographic approaches to help delineate the precise mechanism by which Ldb factors influence SLK activity.

We have recently shown that SLK activity is induced in a scratch wound migration model and that SLK activity is required for cell migration (Wagner *et al*., 2008). If the Ldb molecules are inhibitors of SLK activity then their ablation would be predicted to enhance cell migration. Indeed, deletion of Ldb1 and partial loss of Ldb2 both result in an approximately twofold enhancement of cell migration in Boyden chamber migration assays. When both Ldb molecules are ablated, a 3.5-fold enhancement in migration is observed (Figure 6D). A simultaneous knock down of SLK under those conditions results in normal migration rates, suggesting that the effect of the Ldbs on cell motility are SLK dependent. Consistent with a role for Ldb molecules in negative regulation of SLK activity, siRNA-mediated deletion of Ldb1 resulted in accelerated focal adhesion turnover dynamics in a nocodazole washout experiment (Figure 8A). This is supported by live imaging analysis with GFP-paxillin demonstrating accelerated focal adhesion turnover in cells depleted of Ldb1 by siRNA.

Although likely to be very complex, our data suggest that direct Ldb1/2 association with SLK can regulate kinase activity. This association seems to be subject to complex and dynamic stoichiometry. We speculate that during cell migration, modification of the complex results in altered kinase activity, increased focal contact turnover and migration. The SLK-dependent signaling pathways that are modulated by this system await the identification of SLK substrates.

ACKNOWLEDGMENTS

We thank Kim Wong and Doris Parolin for valuable help with confocal microscopy and live imaging. This work was supported by the Canadian Institute for Health Research, MDAUSA, the Canadian Breast Cancer Foundation, and a Premier's Research for Excellence Award. C.J.S. is the recipient of a Canadian Heart and Stroke Foundation Fellowship. L.A.S. is the recipient of a Canadian Institutes of Health Research scholar award. P. O. and S. W. are the recipients of Ontario Graduate Scholarships in Science and Technology and Natural Sciences and Engineering Research Council studentships, respectively.

REFERENCES

Agulnick, A. D., Taira, M., Breen, J. J., Tanaka, T., Dawid, I. B., and Westphal, H. (1996). Interactions of the LIM-domain-binding factor Ldb1 with LIM homeodomain proteins. Nature *384*, 270–272.

Bach, I., Carriere, C., Ostendorff, H. P., Andersen, B., and Rosenfeld, M. G. (1997). A family of LIM domain-associated cofactors confer transcriptional synergism between LIM and Otx homeodomain proteins. Genes Dev. *11*, 1370–1380.

Brown, M. C., and Turner, C. E. (2002). Roles for the tubulin- and PTP-PEST-binding paxillin LIM domains in cell adhesion and motility. Int. J. Biochem. Cell Biol. *34*, 855–863.

Etienne-Manneville, S., and Hall, A. (2001). Integrin-mediated activation of Cdc42 controls cell polarity in migrating astrocytes through PKCzeta. Cell *106*, 489–498.

Fernandez-Funez, P., Lu, C. H., Rincon-Limas, D. E., Garcia-Bellido, A., and Botas, J. (1998). The relative expression amounts of apterous and its co-factor dLdb/Chip are critical for dorso-ventral compartmentalization in the *Drosophila* wing. EMBO J. *17*, 6846–6853.

Jurata, L. W., Kenny, D. A., and Gill, G. N. (1996). Nuclear LIM interactor, a rhombotin and LIM homeodomain interacting protein, is expressed early in neuronal development. Proc. Natl. Acad. Sci. USA *93*, 11693–11698.

Matthews, J. M., and Visvader, J. E. (2003). LIM-domain-binding protein 1, a multifunctional cofactor that interacts with diverse proteins. EMBO Rep. *4*, 1132–1137.

Mizunuma, H., Miyazawa, J., Sanada, K., and Imai, K. (2003). The LIM-only protein, LMO4, and the LIM domain-binding protein, LDB1, expression in squamous cell carcinomas of the oral cavity. Br. J. Cancer 88, 1543–1548.

Mukhopadhyay, M., *et al*. (2003). Functional ablation of the mouse Ldb1 gene results in severe patterning defects during gastrulation. Development *130*, 495–505.

Nishita, M., Tomizawa, C., Yamamoto, M., Horita, Y., Ohashi, K., and Mizuno, K. (2005). Spatial and temporal regulation of cofilin activity by LIM kinase and Slingshot is critical for directional cell migration. J. Cell Biol. *171*, 349–359.

O'Reilly, P. G., Wagner, S., Franks, D. J., Cailliau, K., Browaeys, E., Dissous, C., and Sabourin, L. A. (2005). The Ste20-like kinase SLK is required for cell cycle progression through G2. J. Biol. Chem. *280*, 42383–42390.

Pike, A.C., Rellos, P., Niesen, F. H., Turnbull, A., Oliver, A. W., Parker, S. A., Turk, B. E., Pearl, L. H., and Knapp, S. (2008). Activation segment dimerization: a mechanism for kinase autophosphorylation of non-consensus sites. EMBO J. *27*, 704–714.

Rincon-Limas, D. E., Lu, C. H., Canal, I., and Botas, J. (2000). The level of DLDB/CHIP controls the activity of the LIM homeodomain protein apterous: evidence for a functional tetramer complex in vivo. EMBO J. *19*, 2602–2614.

Sabourin, L. A., and Rudnicki, M. A. (1999). Induction of apoptosis by SLK, a Ste20-related kinase. Oncogene *18*, 7566–7575.

Sabourin, L. A., Tamai, K., Seale, P., Wagner, J., and Rudnicki, M. A. (2000). Caspase 3 cleavage of the Ste20-related kinase SLK releases and activates an apoptosis-inducing kinase domain and an actin-disassembling region. Mol. Cell. Biol. *20*, 684–696.

Storbeck, C. J., Daniel, K., Zhang, Y. H., Lunde, J., Scime, A., Asakura, A., Jasmin, B., Korneluk, R. G., and Sabourin, L. A. (2004). Ste20-like kinase SLK displays myofiber type specificity and is involved in C2C12 myoblast differentiation. Muscle Nerve *29*, 553–564.

Thaler, J. P., Lee, S. K., Jurata, L. W., Gill, G. N., and Pfaff, S. L. (2002). LIM factor Lhx3 contributes to the specification of motor neuron and interneuron identity through cell-type-specific protein-protein interactions. Cell *110*, 237–249.

van Meyel, D. J., O'Keefe, D. D., Thor, S., Jurata, L. W., Gill, G. N., and Thomas, J. B. (2000). Chip is an essential cofactor for apterous in the regulation of axon guidance in *Drosophila*. Development *127*, 1823–1831.

Wagner, S., Flood, T. A., O'Reilly, P., Hume, K., and Sabourin, L. A. (2002). Association of the Ste20-like kinase (SLK) with the microtubule. Role in Rac1-mediated regulation of actin dynamics during cell adhesion and spreading. J. Biol. Chem. *277*, 37685–37692.

Wagner, S., Storbeck, C. J., Roovers, K., Chaar, Z. Y., Kolodziej, P., McKay, M., and Sabourin, L. A. (2008). FAK/src-family dependent activation of the Ste20-like kinase SLK is required for microtubule-dependent focal adhesion turnover and cell migration. PLoS ONE *3*, e1868.

Webb, D. J., Donais, K., Whitmore, L. A., Thomas, S. M., Turner, C. E., Parsons, J. T., and Horwitz, A. F. (2004). FAK-Src signalling through paxillin, ERK and MLCK regulates adhesion disassembly. Nat. Cell Biol. *6*, 154–161.